

# Fourier-Transform EPR at High-Field/High-Frequency (3.4 T/95 GHz) Using Broadband Stochastic Microwave Excitation

Michael Fuhs, Thomas Prisner,\* and Klaus Möbius

*Institut für Experimentalphysik, Freie Universität Berlin, Arnimallee 14, D-14195 Berlin, Germany; and \*Institut für Physikalische und Theoretische Chemie, Johann-Wolfgang-Goethe-Universität, Marie-Curie-Strasse 11, D-60439 Frankfurt, Germany*

Received September 11, 2000; revised November 28, 2000

**Stochastic excitation with a full-width-half-maximum bandwidth of 250 MHz was used to perform Fourier-transform (FT) high-field/high-frequency electron paramagnetic resonance (EPR) at 3.4T/95 GHz (W-band). Thereby, the required microwave peak power is reduced by a factor of  $\tau_p/T_1$  as compared to equivalent pulsed FT EPR in which the spin system with spin-lattice relaxation time  $T_1$  is excited by a single microwave pulse of length  $\tau_p$ . Stochastic EPR is particularly interesting under high-field/high-frequency conditions, because the limited output power of mm microwave sources, amplifiers, and mixers makes pulse FT EPR in that frequency domain impossible, at least for the near future. On the other hand, FT spectroscopy offers several advantages compared to field-swept magnetic resonance methods, as is demonstrated by its success in NMR and X-band EPR. In this paper we describe a novel stochastic W-band microwave bridge including a bimodal induction mode transmission resonator that serves for decoupling the microwave excitation and signal detection. We report first EPR measurements and discuss experimental difficulties as well as achieved sensitivity. Moreover, we discuss future improvements and the possibility for an application of stochastic W-band FT EPR to transient signals such as those of photoexcited radical pairs in photosynthetic reaction centers.** © 2001 Academic Press

cw and pulse high-field EPR, the spectra are recorded *via* a magnetic field sweep. On the other hand, it is known from NMR or X-band EPR (0.34 T/9.5 GHz) that Fourier-transform (FT) spectroscopy, in which the total spin system is excited by one radiofrequency or microwave pulse and the system response is detected in the time domain, offers several distinct advantages. Among them is the feasibility of measuring correlations between two spins. Two-dimensional correlation spectroscopy (COSY) measurements allow one, for instance, to distinguish resonances belonging to the same individual molecule from those belonging to different molecules (18). Other advantages are the multiplex effect which may lead to enhanced sensitivity and the resolution of Larmor frequencies rather than of magnetic resonance fields. In high-field EPR, magnetic resonance fields are difficult to measure to high accuracy because of nonlinearities in the field sweeps of superconducting magnets. Moreover, homogeneous NMR magnets for high fields that could be used also for EPR do not have the option for a field sweep at all, which makes FT methods even more interesting.

For good sensitivity in pulse EPR one has to turn the magnetization by 90° with one pulse. The bandwidth of this coherent excitation has the approximate magnitude of the reciprocal pulse length that depends on the available microwave power. Most high-frequency microwave sources with good noise characteristics do not supply enough power for such a coherent broadband excitation. For W-band EPR spectrometers (3.4 T/95 GHz) the maximum output powers vary between 6–9 dBm (4–8 mW) when using the nonamplified output of mixers (converting a lower intermediate frequency to 95 GHz) (9) and 14–23 dBm (25–250 mW) when using either amplification (2, 10) or the output of a 95-GHz klystron (5). In the latter case, depending on the quality factor and the conversion factor of the resonator with sample, 90° pulse lengths of about 40 ns can be achieved. This corresponds to an excitation bandwidth of 25 MHz, which is still much smaller than the typical spectral widths of about 280 MHz (10 mT) of interesting biological samples containing, for instance, quinone or tyrosyl radicals. Only with very complex and expensive mm microwave sources, such as extended interaction oscillators, is it possible to obtain output powers of 54 dBm (300 W) and pulse bandwidths of the required

## 1. INTRODUCTION

One of today's main developments of electron paramagnetic resonance (EPR) is directed toward the use of higher magnetic fields and correspondingly higher microwave frequencies (1–10), for example, when EPR is applied for studies of protein structure and dynamics (11–17). Reasons for this trend to higher fields and frequencies are increase in spectral resolution, increase in sensitivity for small samples, information on molecular motion at shorter time scales, and the accessibility of larger zero-field fine-structure splittings. So far, most EPR experiments are performed by measuring either the absorption of continuously (cw) irradiated monochromatic microwaves or the amplitude of a spin echo after two resonant microwave pulses. Especially for high-frequency EPR, with its low available excitation power, the spectral bandwidths of the pulses usually are small compared to the spectrum of the samples. Therefore, in both cases,

magnitude (4). Then, however, the handling of the high power and the loss of signal intensity, owing to the dead time of the EPR resonator and the saturation of the detector, may cause severe problems.

To overcome these difficulties we tried an alternative approach by using a broadband incoherent continuous microwave irradiation (noise) with a spectral bandwidth of about 250 MHz. This *stochastic resonance* corresponds to optical interferometry, and was introduced to NMR by Ernst (19) and Kaiser (20). They showed theoretically and experimentally that the achievable sensitivity for measuring one-dimensional spectra equals that of pulse FT spectroscopy. Therefore, the sensitivity principally is higher than that with conventional cw spectroscopy because of the multiplex effect. Ziessow and Blümich (21, 22) pioneered the stochastic NMR application to the nonlinear system response and showed that the information content of the nonlinear response, obtained by higher order cross-correlation of input and output signals, equals that of multidimensional pulse spectroscopy. More recently, stochastic excitation was also used for X-band EPR (23) and solid-state NMR (24). Besides the application in magnetic resonance, stochastic resonance was reported from other fields, for instance, from microwave rotational absorption spectroscopy (25) and high-resolution optical spectroscopy (26). For low microwave power, the linear response of the spin system,  $k(\sigma)$ , which is the one-pulse response function, is obtained by cross-correlating input,  $x(t)$ , and output,  $y(t)$ , signals

$$k(\sigma) = \int_0^{\infty} y(t)x(t - \sigma) dt. \quad [1]$$

Subsequent Fourier transformation of the cross-correlation yields the spectrum  $K(\omega)$  in the frequency domain. For easier calculation, one usually multiplies the Fourier-transformed and complex-conjugated input function  $\bar{X}(\omega)$  with the Fourier-transformed output function  $Y(\omega)$  in order to obtain  $K(\omega)$ . For optimum sensitivity in stochastic resonance, one has to apply the same average power as in pulse FT spectroscopy. Consequently, for stochastic resonance with continuous microwave irradiation, one needs only peak powers that are reduced by a factor of  $\tau_p/T_1$  compared to pulse spectroscopy, where  $\tau_p$  is the pulse length and  $T_1$  is the spin-lattice relaxation time. This reduction factor,  $\tau_p/T_1$ , contains the ratio of the duty cycles of pulse and stochastic spectroscopy and may be as small as  $10^{-2}$  to  $10^{-3}$ . Thus, optimum excitation power for stochastic EPR depends on the excitation bandwidth  $\nu$  and on  $T_1$ , and is given by (see Ref. (19))

$$B_1^{\text{opt}} = 2\nu/T_1\gamma_e^2. \quad [2]$$

It is this requirement of only relatively low excitation power that makes stochastic resonance particularly interesting for high-field EPR.

Compared to the previously realized stochastic NMR at 280 MHz, with spectral bandwidths up to 200 kHz, stochastic W-band EPR operates at 95 GHz, and typical samples require one to cover a bandwidth of about 250 MHz. Thus the frequency spread to be covered is three orders of magnitude larger than that in NMR. This large bandwidth requirement poses severe experimental problems and, to our knowledge, the only stochastic EPR experiments reported so far were performed at X-band frequencies with a bandwidth of 80 MHz (23). They were realized using analog real-time cross-correlation methods, where the response is fed into an analog mixer together with the delayed excitation. Therefore, the measurement had to be repeated for each cross-correlation delay  $\sigma$ , in analogy to the optical measurements with different path lengths when using a Michelson interferometer. In contrast to these analog experiments, we now digitize the whole time trace of the response of the spin system. Afterward, the cross-correlation with the excitation is performed with a computer in order to gain the multiplex advantage of FT spectroscopy.

In this paper we describe the stochastic excitation method, the new stochastic W-band microwave bridge, and the new bimodal induction mode transmission resonator, before we report on the first FT measurements in high-field EPR. Furthermore, we discuss future improvements of the stochastic W-band EPR experiment as well as the possibility for future applications to photoexcited transient radical pairs in photosynthetic reaction centers.

## 2. EXPERIMENTAL SETUP

The schematic diagram of the experimental setup is shown in Fig. 1. Similar to other realizations of stochastic resonance (19, 20, 23), the broadband microwave excitation is generated by using pseudostochastic maximum-length binary sequences (MLBS) (27), by which the 95-GHz carrier is phase-modulated. MLBS are periodic sequences of binary numbers (0 and 1). The spectral density is similar to that of a pulse train with the same repetition rate and with a pulse length corresponding to the minimum phase bit length,  $\tau_p$ , of the MLBS. In our case,  $\tau_p = 4$  ns, and the resulting excitation bandwidth is 250 MHz (FWHM). The MLBS are generated in the computer that controls the experiment and that is used to program the pulse programmer (Tektronix HFS9003). This unit also triggers the digitizer (Tektronix TDS 744A) each time it repeats the MLBS. Because the MLBS are periodic, the signal can be averaged in order to improve the signal-to-noise ratio. When using pseudostochastic MLBS for excitation, one can perform the data analysis also by applying the Hadamard transformation instead of cross-correlation and subsequent Fourier transformation (28). Therefore this approach is sometimes called Hadamard spectroscopy (28, 29). In our case, the setup can be easily changed for using real stochastic instead of pseudostochastic excitation. This will be necessary when applying the stochastic EPR spectroscopy to rapidly changing transient states and to nonlinear responses.

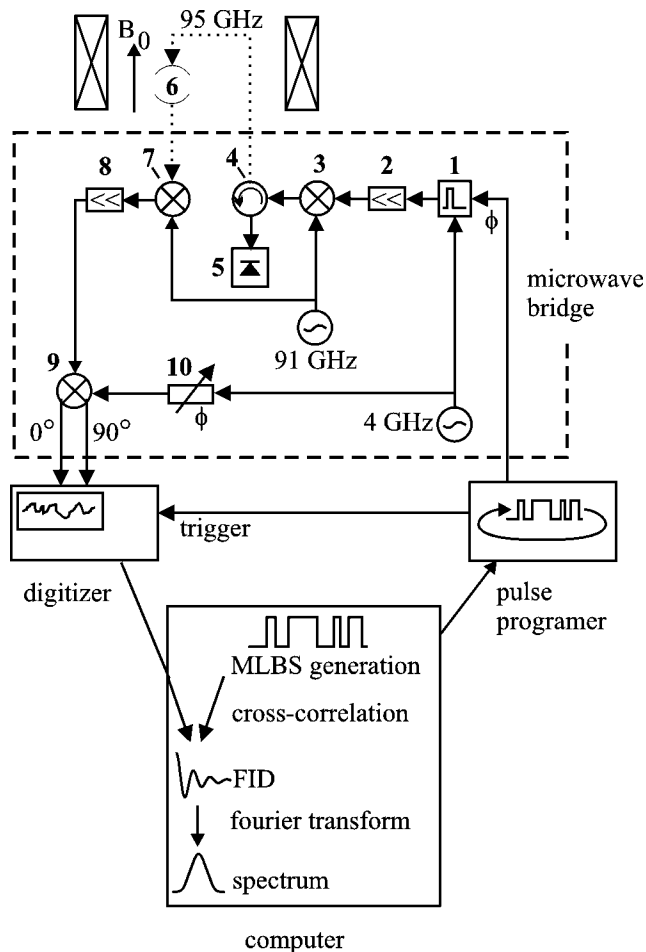


**FIG. 1.** Setup of the stochastic W-band EPR experiment. Dotted line, oversized Ka-band waveguide (see Fig. 2); 1, 4-GHz phase modulator; 2, 4-GHz amplifier; 3, up-converter to 95 GHz; 4, circulator; 5, detection diode; 6, resonator (see Fig. 2); 7, 95-GHz mixer; 8, 4-GHz amplifier; 9, 4-GHz mixer; 10, 4-GHz phase shifter. For details, see text.

Because sufficiently fast 95-GHz phase modulators do not yet exist, we modulate the phase at an intermediate frequency (IF) of 4 GHz (phase modulator Miteq BMA0208LW2) which is then up-converted with the output of a 91-GHz klystron (Varian). The resulting 95-GHz microwave is coupled to the transmission resonator *via* a three-port circulator. On its third port a detection diode is used to observe the power reflected at the resonator in order to check and adjust its resonance frequency. The power into the resonator is limited to 2 dBm by the maximum output of the up-converter (Farran BUC-10). The output signal of the transmission resonator is down-converted by a mixer (Farran BMC-10B) where the 91-GHz local frequency is obtained directly from the klystron. The resulting IF is down-converted with the 4-GHz local frequency in quadrature detection (Miteq IQZ0046) and then recorded with the digitizer. The detection phase is adjusted using the phase shifter in the 4-GHz local branch. Great care was taken to avoid reflections in the microwave bridge because mul-

multiple reflections, e.g., between sample resonator and microwave bridge, lead to standing waves in resonator-like structures of the transmission line, and will therefore limit the required bandwidth. For this reason, the connections between the microwave components are kept as short as possible, and additional isolators are included to reduce standing waves. For the connections of the sample resonator in the cryomagnet to the microwave bridge an oversized rectangular waveguide (Ka-band) is used (dotted line). The ultimately realized length of about 50 cm still leads to a train of modes of standing waves in the waveguides between resonator and circulator as well as between resonator and mixer, separated from each other by 150 MHz. For a large enough bandwidth it is necessary to perform the EPR measurements at the center between two of these modes. The bandwidth of the microwave setup, without sample resonator, was measured to be larger than 250 MHz. The measured overall noise figure of about 11 dB is determined mainly by the noise figure of the 95-GHz microwave mixer used for down-conversion.

The more recent stochastic NMR experiments have been realized by using small-angle pulses with random phase for excitation, after each of which one data point must be sampled. In EPR, because of the required bandwidth of 250 MHz, the time window for one pulse and detection sampling point would be 4 ns. For technical reasons this is far too short. Therefore, in stochastic EPR one has to use continuous irradiation with broadband microwaves instead. One of the severe technical problems of the continuous irradiation scheme is simultaneous excitation and detection and, related to this, the dynamic range of the detector. In our setup the dynamic range is limited by the 8-bit analog/digital converter and the 16-bit data accumulation of the digitizer. When—instead of using a transmission type resonator—a resonator in reflection is used, which is the common strategy in EPR, each phase switching of the exciting microwaves leads to strong reflections at the resonator and concomitant saturation of the detector. This results in artifacts in the cross-correlation. In order to achieve effective decoupling of excitation and detection channels we have built a bimodal induction mode transmission resonator for the sample (Fig. 2). Bimodal induction mode resonators work in two degenerate, linearly polarized orthogonal modes. The linearly polarized excitation is carried by one of them and cannot be observed in the mode orthogonal to that. The circularly polarized EPR signal, however, can be observed in both modes. Therefore, using the orthogonal mode for detection, the EPR signal is separated to a high degree from the background microwave excitation.

The bimodal probehead was realized as a Fabry–Perot resonator operating in the TEM<sub>008</sub> mode with the detection arm rotated by 90° with respect to the excitation arm (see Fig. 2A). The gold-plated brass mirrors (diameter 19 mm, curvature  $R = 15$  mm) are positioned in a brass tube. The resonator is normally overcoupled in order to decrease the quality factor to 200 and, thereby, to obtain the required high bandwidth. The microwave coupling can be varied by using mirrors with irises of different diameter ( $\varnothing 0.9$  mm– $\varnothing 1.2$  mm). The sample is introduced

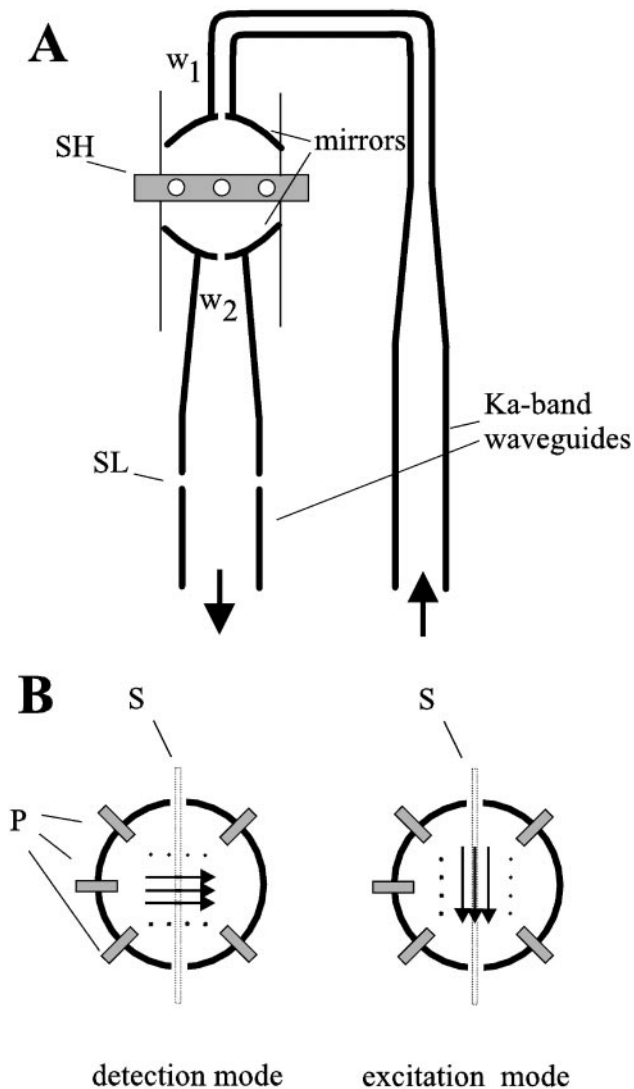


**FIG. 2.** W-band bimodal induction mode transmission Fabry-Perot resonator. (A) The two linearly polarized TEM<sub>008</sub> modes are coupled by the two W-band waveguides perpendicular to each other, indicated by  $w_1$  for excitation and  $w_2$  for detection. The connection to the microwave bridge is made by two oversized Ka-band waveguides. In the detection arm the waveguide is slit (SL) to allow for stress-free frequency adjustment. The two mirrors are kept in position in a brass tube that also holds the sample and paddle holder (SH). (B) Sectional view through the sample and paddle holder (SH) in the center plane. The solid arrows depict the magnetic microwave field direction  $B_1$  of the two linearly polarized modes. The dots indicate the electric component of the microwave field. The left side shows the mode used for detection, and the right side that for excitation. The sample (S) is introduced along the magnetic field lines of the excitation mode. Three to five brass screws were used as paddles (P) to increase the decoupling of the two modes.

either as a film on the surface of one of the two mirrors, or in sample tubes ( $\varnothing 0.7$  mm for toluene) in the center plane of the resonator along the polarization axis of one of the two modes. For frequency adjustment one of the mirrors can be moved vertically. To enable this motion the waveguide is slit. Unwanted reflections are negligible as long as the slit does not exceed

0.1 mm. By this construction an adjustable frequency range of 1 GHz can be achieved. The microwave field  $B_1$  at the center of the critically coupled resonator (quality factor  $Q$ ) is related to the incident microwave power  $P_{mw}$  by the conversion factor  $c = B_1/\sqrt{P_{mw}Q}$ . With the conversion factor  $3.3 \mu\text{T}/\sqrt{\text{W}}$ , as determined for a similar reflection type Fabry-Perot resonator (3), and the output power of our W-band setup, a maximum  $B_1$  field of  $1.8 \mu\text{T}$  can be achieved.

The decoupling of excitation and detection of such a resonator is usually not better than 20 dB. It is possible to increase the decoupling by twisting the two orthogonal waveguides somewhat with respect to each, as was done for the 140-GHz bimodal resonator in Ref. (4). To avoid the mechanical stress on the waveguides due to this twisting, we instead increased decoupling by adjusting conducting screws (brass,  $\varnothing 2$  mm) in the center plane of the resonator. These screws work in analogy to the “paddles” in the bimodal cylindrical cavities used in X-band (30, 31). They act as additional capacitance and correct for deviations from optimum geometry and for field distortions by the sample. From X-band cylindrical cavities it is known that, for optimum decoupling of the two modes, four metallic and two resistive screws have to be introduced at well-defined positions in the TE<sub>111</sub> mode (30). Since in a Fabry-Perot resonator the field geometry is rather different, the same paddle configuration is less efficient. Nevertheless, it was possible to increase the decoupling to 60 dB in a narrow band of about 20 MHz and to 40 dB in a broad band of about 500 MHz by adjusting two to five brass screws according to Fig. 2B.

### 3. RESULTS

As a test sample, we used a nitroxide-nitronyle radical dissolved in toluene to a concentration of 1 mmol. The structure of this radical is given in Fig. 3A. For stochastic excitation we used a MLBS with a length of 511 bits,  $\tau_p = 4$  ns time base, and, consequently, a period of  $2.04 \mu\text{s}$ . The output from the resonator was recorded both with the magnetic  $B_0$  field setting close to the resonant field and with  $B_0$  far off resonance, in order to obtain an off-resonance baseline which was then subtracted from the signal. Each measurement consists of 70,000 accumulations, which leads to a total accumulation time of only  $70,000 \times 2.04 \mu\text{s} = 0.14$  s. Nevertheless, because of the limited duty cycle of our digitizer, it took about 7 min to perform the measurement. Figure 3B depicts the cross-correlation of the MLBS and the signal obtained in the way described above. The first 5 ns is distorted due to source noise and imperfect baseline correction. These distortions have been corrected with a linear prediction routine, written in Matlab program language, following the algorithm in Ref. (32). Subsequent Fourier transformation results in the absorptive and dispersive spectra. As seen in Fig. 3C, all the expected five hyperfine lines from the  $^{14}\text{N}$  nuclei in the five-membered ring of the nitroxide-nitronyle radical could be resolved over a spectral width of 90 MHz (3 mT) with one single experiment, i.e., at one fixed  $B_0$  value.

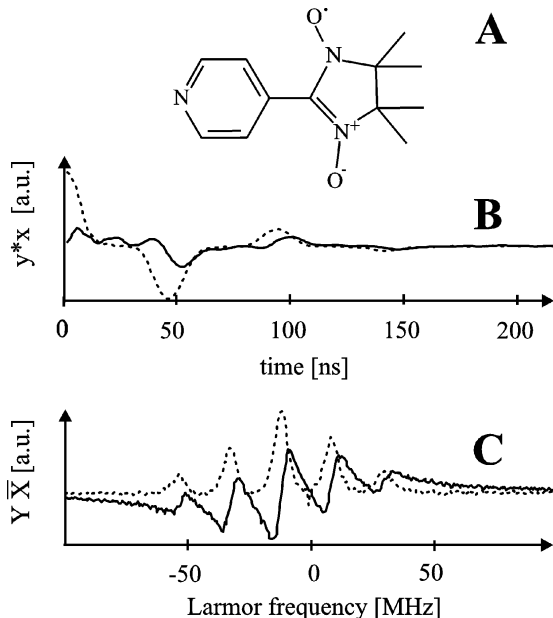


**FIG. 3.** Stochastic W-band EPR on a nitroxide-nitronyle radical. (A) Molecular structure. (B) Cross-correlation of input and output signals,  $x(t)$  and  $y(t)$  in the  $0^\circ$  (full line) and  $90^\circ$  (dotted line) detection channels. The data of the first 5 ns were corrected using linear prediction. (C) Absorption (dotted line) and dispersion (full line) spectra after Fourier transformation.

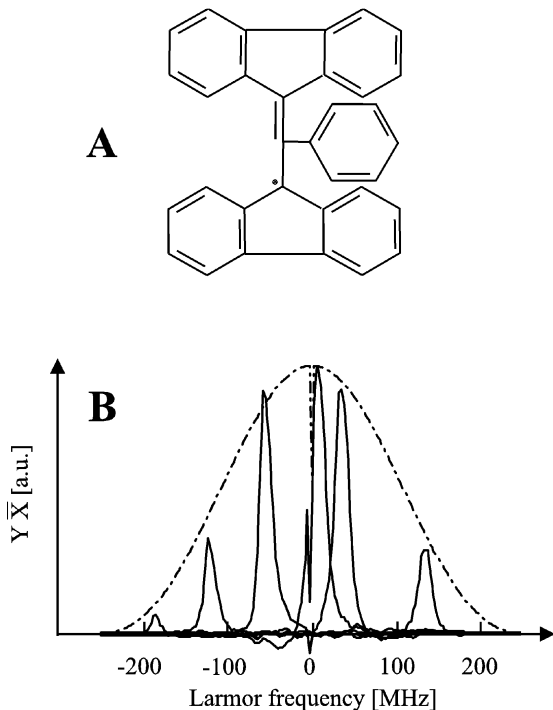


**FIG. 4.** (A) Molecular structure of the BDPA radical. (B) Stochastic W-band EPR absorption spectra (full lines) at different magnetic  $B_0$  fields, i.e., measured with different Larmor frequencies. The dotted line (---) shows the spectral density ( $|X(\omega)|^2$ ) of the stochastic excitation. There is a blind spot at zero frequency. The separation of two Fourier components of the excitation, due to the periodicity of the MLBS, is 490 kHz.

A spin probe with unresolved (proton) hyperfine structure was used to measure the actual spectral density of the microwave excitation and detection channels. BDPA ( $\alpha,\gamma$ -bisdiphenylene- $\beta$ -phenylallyl; see Fig. 4A) shows a single Gaussian EPR line of an inhomogeneously broadened width of about 1 mT. BDPA was dissolved in toluene together with polystyrene and dried and placed in the resonator as a film on one of the two mirrors. The number of spins in the resonator was about  $2 \times 10^{16}$ . In Fig. 4B the stochastic FT EPR spectra are shown for different values of the  $B_0$  field. Because the Larmor frequency is proportional to  $B_0$ , the signal amplitude  $Y\bar{X}$  (Fourier transform of the cross-correlation) is directly related to the spectral density of the microwave MLBS excitation,  $|X(\omega)|^2$ , that is shown as a dotted line in Fig. 4B. Around the center frequency, this relation is well reproduced in the experiment, but at the wings the signal intensity is slightly smaller. The reason for this is that the resonance frequencies of the two orthogonal modes of the resonator were not exactly equal. Optimum overlap of the two modes depends very critically on the adjustment of the brass screws (paddles) that were used to obtain maximum decoupling of the two modes.

#### 4. DISCUSSION

The sensitivity of cw EPR spectrometers is usually expressed as the minimum number of spins,  $N_{\min}$ , with a linewidth of 1 mT that can be detected with a signal-to-noise ( $S/N$ ) ratio of 1 at a detector bandwidth of 1 Hz (33). Because it does not make sense to normalize Fourier-transform measurements to a detector bandwidth, instead one has to consider the required measuring times in order to compare stochastic sensitivity with cw sensitivity. For a given detector bandwidth,  $\Delta f_{\text{cw}}$  in hertz, the cw measuring time,  $T_{\text{cw}}$ , depends on the sweep range and resolution,  $\nu$  and  $\Delta\nu$  in linear frequency units:  $T_{\text{cw}} = \nu / \Delta\nu \Delta f_{\text{cw}}$ . Therefore,  $N_{\min}$  for the stochastic EPR experiment is calculated as the minimum number of spins detected with a  $S/N$  of 1 when measured with the same measuring time required for a cw spectrum with the same spectral parameters,

$$N_{\min} = \frac{N}{(S/N)_{\text{exp}} \Delta B n} \sqrt{\frac{T_{\text{exp}}}{T_{\text{cw}}}}, \quad [3]$$

with the EPR linewidth  $\Delta B$ , the number  $n$  of resolved hyperfine lines, the number  $N$  of spins in the resonator, and the measuring time  $T_{\text{exp}}$  of the stochastic experiment. We want to cover a spectral range of 14 mT, i.e.,  $\nu = 390$  MHz (half-width of spectral density is 250 MHz), and the stochastic spectra were recorded with a resolution of  $\Delta\nu = 0.5$  MHz. Because of the  $(\sin \nu / \nu)^2$  shape of the spectral density of stochastic excitation, the sensitivity depends on the off-resonance position of the EPR signal, which determines the offset between the Larmor frequency and that of the microwave carrier,  $\nu_{\text{MW}}$ . We determined the sensitivity for a Larmor frequency of  $\nu_{\text{MW}} \pm 50$  MHz. Hence, for the nitroxide-nitronyle sample, we obtained  $N_{\min} = 4 \times 10^{13}$  spins/

mT, and for the BDPA sample  $N_{\min} = 8 \times 10^{13}$  spins/mT. These two values are in good agreement with each other when taking into account the uncertainties in measuring concentrations and  $S/N$  ratios.

The theoretical sensitivity limit is given by the comparison of thermal noise and signal intensity. There are mainly two limitations for the sensitivity of our setup. (i) The microwave field/power conversion factor of the Fabry–Perot resonator is 10–15 times smaller than that of a cylindrical cavity, and a  $B_1$  field of only  $1.8 \mu\text{T}$  is reached. The sensitivity for an unsaturated signal depends quadratically on the conversion factor. Although stochastic EPR does not require high  $B_1$  fields, this value of  $1.8 \mu\text{T}$  is still small compared to the optimum value, that is calculated to be  $180 \mu\text{T}$ . This optimum value follows from Eq. [2] for a typical spin system with a spin–lattice relaxation time of  $1 \mu\text{s}$  and an excitation bandwidth used in our experiments. (ii) The digitizer available to us triggers only every 10 ms, but the length of the recorded time traces is  $2.04 \mu\text{s}$ . Consequently, we can measure only with a very low duty cycle of about  $2 \times 10^{-4}$ . Taking these limitations into account, the theoretical thermal noise limit of our stochastic spectrometer for not-saturated samples is  $N_{\min}^{\text{theo}} = 3 \times 10^{13}$  spins/mT. This value was calculated using Feher’s expressions for cw EPR sensitivity (33) and Ernst’s expressions for comparison of cw and stochastic magnetic resonance sensitivities (19). In our case, far off saturation, both methods give the same theoretical sensitivity. The determined experimental sensitivity is very close to the theoretical value. This means that for the stochastic measurements the noise is determined mainly by the thermal noise of the microwave mixer. Thus, the noise floor is not drastically affected by source noise and artifacts that might arise from fast phase switching and data sampling. Close to the carrier frequency the source noise showed up in an imperfect baseline correction. This leads to distortions during the first 5 ns of the cross-correlation. Nevertheless, these remaining distortions must be compared with the dead-time distortions in pulsed EPR. They are generally much larger because of saturating the detector by the high-power microwave pulses.

## 5. OUTLOOK

On the basis of the preliminary results presented, we now discuss future possibilities of the high-field/high-frequency stochastic EPR method. So far its sensitivity is smaller than that in cw EPR with a cylindrical cavity. This is due to the small duty cycle of the stochastic experiment and the small conversion factor of the Fabry–Perot resonator. The duty cycle could be increased by using a faster averaging digitizer, which would lead to an increase of sensitivity by about two orders of magnitude. On the other hand, when performing an experiment with pulsed light excitation of the sample, the effective duty cycle is determined by the repetition rate of the laser. In this case, the duty cycle of the corresponding cw experiment is as low as that of the stochastic EPR. Therefore, the low duty cycle is not a principal limitation of stochastic EPR. Concerning the small

conversion factor, we used a Fabry–Perot bimodal resonator because of relative ease of its construction. We believe, however, that it should be possible to build also a W-band bimodal cylindrical transmission cavity, following the known X-band design (30). In this design, one mode is coupled through the front, and the other one through the side of the cylinder. In contrast to this, in a W-band cylindrical cavity one probably would have to couple both modes through the front plates because coupling through the side would require extreme accuracy in centering the bore. A bimodal cylindrical cavity has two major advantages: First, the conversion factor is increased by more than one order of magnitude, resulting in an increase of sensitivity by two orders of magnitude (the sensitivity depends quadratically on the conversion factor). Second, in such a cylindrical cavity the adjustment of decoupling the two modes, by introducing resistive and capacitive screws in the middle plane, is expected to work better than in the Fabry–Perot resonator. Moreover, by amplifying the excitation power by 10 dB (which should be technically feasible in the near future) one would approach the optimum excitation power for samples with relaxation times of about  $1 \mu\text{s}$ . On the other hand, even without changing our present setup, we reach optimum microwave power for spin systems with relaxation times longer than 10 ms. This is rather common for cooled samples. Thus, with the  $B_1$  field close to the optimum value, one can even expect to observe also nonlinear responses.

This would be particularly interesting for the investigation of biradicals or light-induced radical pairs, such as those occurring in photosynthetic reaction centers (15). The nonlinear responses contain information about the correlation of the two electron spins. Therefore, they provide additional resolution for spin connectivities between different parts of spectra which, in return, can be used to determine distances and orientations of the two radical pair partners. Transient systems, after light excitation, are often spin-polarized, i.e., neither time invariant nor in thermal equilibrium. It is known that in this case large flip angles of pulsed EPR would lead to spectra with significant line distortions (34). In contrast to pulsed EPR with large flip angles, stochastic EPR could also be applied to spin-polarized systems without suffering from line distortions. This is valid because the small microwave power used for stochastic resonance corresponds to small flip angles in pulsed spectroscopy. However, the decay time constants of the spin polarization should be larger than the period of the MLBS used. When this is not the case, artifacts may appear. Simulations show that, in order to average them to zero, one has to apply several, i.e., 30–100, different sequences of binary noise and subsequently average the cross-correlations. This procedure would require only small changes in the computer control of our present experimental setup. The same must be done for investigating the nonlinear responses (22).

Whether high-field/high-frequency stochastic EPR is an alternative to pulsed Fourier-transform EPR will depend on future developments of high-power microwave sources and amplifiers in the mm and sub-mm region. When going to frequencies even

higher than 95 GHz, where powerful low-noise sources will probably remain inaccessible in the near future, one could think of using the source noise directly for stochastic excitation and performing cross-correlation in analogy to what is done in dispersive infrared interferometry (35).

### ACKNOWLEDGMENTS

We thank J. Törring (Frankfurt/Berlin) for programing the computer control of the experiment and for helpful discussions about the experiment. We thank S. Yamauchi (Sendai) for providing us with the nitroxide-nitronyle sample. This work was supported by the Deutsche Forschungsgemeinschaft (SPP 1051, SFB 498).

### REFERENCES

- O. Grinberg, A. A. Dubinskii, and Y. S. Lebedev, Electron paramagnetic resonance of free radicals in the two-millimetre wavelength range, *Russ. Chem. Rev. (Engl. Transl.)* **52**, 850–865 (1983).
- R. T. Weber, J. A. M. Disselhorst, L. J. Prevo, J. Schmidt, and W. T. Wenckebach, Electron-spin-echo spectroscopy at 95 GHz, *J. Magn. Reson.* **81**, 129–144 (1989).
- O. Burghaus, M. Rohrer, T. Götzinger, M. Plato, and K. Möbius, A novel high-field/high-frequency EPR and ENDOR spectrometer operating at 3 mm wavelength, *Meas. Sci. Technol.* **3**, 765–774 (1992).
- T. F. Prisner, S. Un, and R. G. Griffin, Pulsed ESR at 140 GHz, *Isr. J. Chem.* **32**, 357–353 (1992).
- T. F. Prisner, M. Rohrer, and K. Möbius, Pulsed 95 GHz high-field EPR heterodyne spectrometer, *Appl. Magn. Reson.* **7**, 167–183 (1994).
- K. A. Earle, D. S. Tipikin, and J. H. Freed, Far-infrared electron-paramagnetic-resonance spectrometer using a quasioptical reflection bridge, *Rev. Sci. Instrum.* **67**, 2502–2513 (1996).
- P. J. Bratt, M. Rohrer, J. Krzystek, M. C. W. Evans, L. C. Brunel, and A. Angerhofer, Submillimeter high-field EPR studies of the primary donor  $P_{700}^{+}$  in plant photosystem I, *J. Phys. Chem. B* **101**, 9686–9689 (1997).
- E. J. Reijerse, P. J. van Dam, A. A. K. Klaassen, W. R. Hagen, P. J. M. van Bentum, and G. M. Smith, Concepts in high-frequency EPR—Applications to bio-inorganic systems, *Appl. Magn. Reson.* **14**, 153–167 (1998).
- D. Schmalbein, G. G. Maresch, A. Kamlowski, and P. Höfer, The Bruker high-frequency-EPR system, *Appl. Magn. Reson.* **16**, 185–205 (1999).
- I. Gromov, V. Krymov, P. Manikandan, D. Arieli, and D. Goldfarb, A W-band pulsed ENDOR spectrometer: Setup and application to transition metal centers, *J. Magn. Reson.* **139**, 8–17 (1999).
- K. Möbius, Primary processes in photosynthesis: What do we learn from high-field EPR spectroscopy? *Chem. Soc. Rev.* **29**, 129–139 (2000).
- M. van Gastel, G. W. Canters, H. Krupka, A. Messerschmidt, E. C. de Waal, G. C. M. Warmerdam, and E. J. J. Groenen, Axial ligation in blue-copper proteins. A W-band spin echo detected paramagnetic resonance study of the azurin mutant M121H, *J. Am. Chem. Soc.* **122**, 2322–2328 (2000).
- P. Dorlet, A. Boussac, A. W. Rutherford, and S. Un, Multifrequency high-field EPR study of the interaction between the tyrosyl Z radical and the manganese cluster in plant photosystem II, *J. Phys. Chem. B* **103**, 10945–10954 (1999).
- C. C. Lawrence, M. Bennati, H. V. Obias, G. Bar, R. G. Griffin, and J. Stubbe, High-field EPR detection of a disulfide radical anion in the reduction of cytidine 5'-diphosphate by the E441QR1 mutant of *Escherichia coli* ribonucleotide reductase, *Proc. Natl. Acad. Sci. USA* **96**, 8979–8984 (1999).
- D. Stehlik and K. Möbius, New EPR methods for investigating photoprocesses with paramagnetic intermediates, *Annu. Rev. Phys. Chem.* **48**, 745–784 (1997).
- M. Rohrer, P. Gast, K. Möbius, and T. Prisner, Anisotropic motion of semiquinones in photosynthetic reaction centers of *Rhodobacter sphaeroides* R26 and in frozen isopropanol solution as measured by pulsed high-field EPR at 95 GHz, *Chem. Phys. Lett.* **259**, 523–530 (1996).
- T. F. Prisner, A. van der Est, R. Bittl, W. Lubitz, D. Stehlik, and K. Möbius, Time-resolved W-band (95 GHz) EPR spectroscopy of Zn-substituted reaction centers of *Rhodobacter sphaeroides* R-26, *Chem. Phys.* **194**, 361–370 (1995).
- R. R. Ernst, G. Bodenhausen, and A. Wokaun, “Principles of Nuclear Magnetic Resonance in One and Two Dimensions,” Clarendon Press, Oxford (1987).
- R. R. Ernst, Magnetic resonance with stochastic excitation, *J. Magn. Reson.* **3**, 10–27 (1970).
- R. Kaiser, Coherent spectroscopy with noise signals, *J. Magn. Reson.* **3**, 28–43 (1970).
- B. Blümich and D. Ziessow, Nonlinear noise analysis in nuclear magnetic resonance spectroscopy. 1D, 2D and 3D spectra, *J. Chem. Phys.* **78**, 1059–1076 (1983).
- B. Blümich, White noise nonlinear system analysis in nuclear magnetic resonance spectroscopy, *Prog. NMR Spectrosc.* **19**, 331–417 (1987).
- T. Prisner and K.-P. Dinse, ESR with stochastic excitation, *J. Magn. Reson.* **84**, 296–308 (1989).
- D.-K. Yang, J. E. Atkins, C. C. Lester, and D. B. Zax, New developments in nuclear magnetic resonance using noise spectroscopy, *Mol. Phys.* **5**, 747–757 (1998).
- J. M. Ramsey and W. B. Whitten, Fourier transform microwave spectrometer using an electric-field cross-correlation technique, *Rev. Sci. Instrum.* **57**, 1329–1337 (1986).
- M. P. Winters, C. W. Oates, J. L. Hall, and K. P. Dinse, High-resolution optical multiplex spectroscopy, *J. Opt. Soc. Am. B* **9**, 498–506 (1992).
- S. W. Golomb, “Shift Register Sequences,” Holden-Day, San Francisco, CA (1967).
- R. Kaiser, Application of the Hadamard transform to NMR spectroscopy with pseudonoise excitation, *J. Magn. Reson.* **15**, 44–63 (1974).
- D. Ziessow and B. Blümich, Hadamard-NMR spektroskopie, *Ber. Bunsen-Ges. Phys. Chem.* **78**, 1168–1179 (1974).
- D. Teaney, M. P. Klein, and A. M. Portis, Microwave superheterodyne induction spectrometer, *Rev. Sci. Instrum.* **32**, 721–729 (1961).
- J. S. Hyde, J. C. W. Chien, and J. H. Freed, Electron-electron double resonance of free radicals in solution, *J. Chem. Phys.* **48**, 4211–4226 (1968).
- R. de Beer and D. van Ormondt, Resolution enhancement in the time domain analysis of ESEEM, in “Advanced EPR, Applications in Biology and Biochemistry” (A. J. Hoff, Ed.), pp. 135–176, Elsevier, Amsterdam (1989).
- G. Feher, Sensitivity considerations in microwave paramagnetic resonance absorption techniques, *Bell System Tech. J.* **36**, 449–484 (1957).
- S. Schäublin, A. Höhener, and R. R. Ernst, Fourier spectroscopy of nonequilibrium States, application to CIDNP, Overhauser experiments and relaxation time measurements, *J. Magn. Reson.* **13**, 196–216 (1974).
- P. R. Griffith and J. A. de Haseth, “Fourier Transform Infrared Spectroscopy,” Wiley, New York (1986).